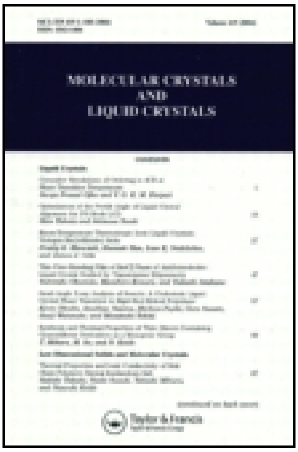

Molecular Crystals and Liquid Crystals
Publication details, including instructions for authors and subscription information:
http://www.tandfonline.com/loi/gmcl20

A Comparison of Pair Potential for Some Polar and Non-Polar Mesogenic Molecules

Shailendar Kumar Thakur [a] & Mihir Roychoudhury [a]
[a] Department of Physics, Deen Dayal Upadhyay Gorakhpur University, Gorakhpur, India

Version of record first published: 30 Jul 2012.

To cite this article: Shailendar Kumar Thakur & Mihir Roychoudhury (2012): A Comparison of Pair Potential for Some Polar and Non-Polar Mesogenic Molecules, Molecular Crystals and Liquid Crystals, 562:1, 28-42

To link to this article: http://dx.doi.org/10.1080/10426507.2012.660863

Mol. Cryst. Liq. Cryst., Vol. 562: pp. 28–42, 2012
Copyright © Taylor & Francis Group, LLC
ISSN: 1542-1406 print/1563-5287 online
DOI: 10.1080/10426507.2012.660863

A Comparison of Pair Potential for Some Polar and Non-Polar Mesogenic Molecules

SHAILENDAR KUMAR THAKUR*
AND MIHIR ROYCHOUDHURY

Department of Physics, Deen Dayal Upadhyay Gorakhpur University,
Gorakhpur, India

Asymmetry of pair potential plays a crucial role in the formation of mesophases in molecular systems. Variation of such asymmetry is closely related to the constituents of the molecules as well as their positions. To investigate the asymmetry as well as its effect on molecular behavior, a few polar biphenyl and non-polar 2,5 disubstituted pyridine derivatives have been chosen. The intermolecular interaction energy between a pair of molecules has been calculated with the help of a standard method as prescribed by Claverie (Claverie, P. (1978). Elaborations of approximate formulas for interactions between large molecules: Applications in organic chemistry. In: B. Pullman (Eds.), *Inter Molecular Interactions from Diatomic to Biopolymers,* J. Wiley & Sons Ltd.: Hoboken, NJ, 217–226.). *Molecular geometry of all the selected systems was fully optimized without any constraint, and the net atomic charge and the dipole moment on each atomic center was calculated using the Gaussian03 program with density functional B3LYP method using 6-31G** as the basis set. The dispersion and the short range repulsion energy terms have been calculated using semiempirical Kitaigorodskii's "6-exp" formula. An attempt has been made to explain the phase sequences on the basis of the ratios of various interaction energy terms.*

Supplemental materials are available for this article. Go to the publisher's online edition of Molecular Crystals and Liquid Crystals *to view the free supplemental file.*

Keywords Gaussian03; intermolecular interaction; mesophases; multicenter-multipole

1. Introduction

Liquid crystals or mesogens are a well-investigated class of molecules among technologists and academicians because of their wide application in high technology devices, particularly displays. These molecules also exhibit the phenomenon of self-organization but are structurally much more simple than biological molecules. Liquid crystals can be subdivided into theromtropic and lyotropic types; the former are more investigated, but the latter are of increasing importance in the biological area. The important, distinguishing feature of liquid crystals is that they retain molecular order to some extent, even in the liquid state, hence the name "liquid crystals" [1–3].

It is now well established that mesogenicity arises due to asymmetry of pair potential [4–6]. Computational studies to understand the behavior of liquid crystalline molecules have been carried out by several workers with different theoretical approaches [7–10]. Now

---

*Address correspondence to Shailendar Kumar Thakur, Department of Physics, Deen Dayal Upadhyay Gorakhpur University, Gorakhpur, India. E-mail: sktup_in@rediffmail.com it is believed that the atomistic modeling of the formation of molecular complexes provides a better insight into the process and mechanism of the formation of mesophases [11–13]. However, all the earlier theoretical approaches aimed at predicting the bulk properties of the materials with the help of molecular modeling did not address directly the reasons for mesogenic behavior at an atomic level and why a minor change in molecular constituent changes the phase behavior [14]. Recently G. Tiberio et al. used atomistic modeling in attempts to predict the nematic to isotropic phase transition [15].

Due to reasons mentioned above, it was concluded that the best way to deal mesogens at a molecular level is to take up the actual molecular geometry and on the basis of electronic properties calculated using quantum-mechanical methods, the intermolecular interaction energy could be calculated in a stepwise manner. However, since there is no direct method of solving the Schrödinger equation for a polyatomic system, some approximation has to be made. Further there is no single theory to evaluate properties of molecular complexes in terms of individual molecular properties of the interacting molecules. Rayleigh–Schrödinger perturbation theory for long-range interactions appears to be suitable at least for the electrostatic and the polarization parts. For the short-range interaction parts, e.g., dispersion and repulsion, it is convenient to employ semiempirical methods. The aim of the calculation is to take into consideration of the actual geometry of the molecules. The correlation has been made with the asymmetry of pair potential of the selected molecules and the phase behavior of mesogens. So, electronic properties expressed with respect to the atomic positions are desirable. Thus a multicentered-multipole expansion method taking various atoms as a center seems to be a necessity, not only to reduce the computational complexities, but also to include the geometrical features. There are many methods available for the electron population analysis of the molecules. We have employed density functional B3LYP method using 6–31** as a basis set in the present work, as it appears to be the most suitable one for moderate size organic molecules [16].

The strategy of computation of the interaction energy at various configurations of a molecular pair depends on the molecular structure under investigation. The majority of thermotropics either exhibit nematic or smectic character. These molecules are in general of lath shape. The maximum overlap occurs when the plane surfaces come in contact and the molecules are aligned in the same direction. This is termed as stacking. Once stacking is achieved, the two sides in the plane are still open and interaction is still possible from these sides. Such a configuration may be termed as the in-plane interaction. If polar groups are projected outward, contribution to the in-plane interaction may be significant. In a smectic phase, layer formation through in-plane interactions may also be possible; hence, it is also necessary to evaluate the energies of such configurations. The ends of such molecules have very small area for overlapping, but if they contain strong polar groups such as hydroxyl, cyano etc., then strong hydrogen bonding between the molecules is possible resulting in dimer formation. Such strong terminal interactions increase the effective length of the molecule and thereby affect the mesogenic character. It is, therefore, advisable to divide the interactions into three classes namely (1) stacking, (2) in-plane, and (3) terminal. It is computationally efficient and at the same time gives better insight into the mesogenic character. Thus the interaction energy evaluated under the above method may provide a good measure of anisotropy of crystal binding forces.

If the anisotropy is high, the strongest one out of the three possible types of interactions should be capable of retaining the order. It should be noted that configurational specificity is another important factor that must be taken into account. If the configurations obtained by translating or rotating one molecule with respect to the interacting molecule are energetically close, there is always a finite probability of finding the molecule in those configurations.

To decide the mesogenic character, the relative anisotropy and the relative freedom are important factors. In the present work, two classes of molecules have been selected for detailed investigation.

1) Bipolar mesogens represented by the molecules H6CBP and H6NBP, and
2) 2,5-disubsituted pyridine derivatives with non-polar end groups.

Both H6CBP and H6NBP are reported as nematic and are of high melting point. The crystal structure of H6CBP shows two slightly different conformations of the same molecule. This ambiguity does not occur in theoretical calculations as the geometry is optimized before evaluating the interaction energy. Thus, the theoretical calculation uses the most probable conformations of the free molecule [17].

It was realized that bipolar mesogens exhibit nematic character since the terminal interactions are strong and, hence, stacking interactions dominate over the in-plane interactions. In order to examine the smectic character present in the mesogens, it is necessary to select a class of molecule that contains both types, i.e., pure nematogens as well as molecules having a smectic phase followed by a nematic phase. The class of 2,5 disubstituted pyridines seems to be suitable for this purpose. The effect on physicochemical properties of liquid crystals due to the introduction of the pyridine 2,5-diyl fragment into the molecular core had attracted attention of scientists working in the field of liquid crystals. Petrov and Pavluchenko [14] have presented a comparative study of 60 compounds of this class and pointed out some unusual structure–property relationships. It has been observed that in the case of two ring alkyl alkoxyl pyridines, the variation in the length of alkyl chain or the positions of the hetro atoms in the ring affect the mesogenic character significantly. We have selected the three molecules of pyridine derivatives for our study, these are 2-(4′-cyclohexyl-(-4″ pentyl) phenyl-5-ethyl-pyridine (PD-1), 2-(4-cyclohexyl-(4″-ethyl)-phenyl)-5-propyl pyridine (PD-2), and 4-(4′-pentyl)-2′ pyridyl phenyl 4-(enyl)-cyclo hexanoate (PD-3).

2. Methods of Calculation

2.1 Geometry Optimization

The following procedure has been adopted uniformly for all the molecules under investigation.

The molecular geometry was generated using **GaussView.** Geometry optimization, frequency analysis and calculation of electrostatic properties were carried out using the hybrid density functional theory B3LYP with 6-31G** as a basis set using **Gaussian03** [18]. All the structures were fully optimized without any constraints and checked for imaginary frequencies as well.

2.2 Intermolecular Interaction Energy Calculations

Inter molecular interaction energy for a molecular pair was computed using Rayleigh–Schrödinger perturbation theory under a Longuet–Hggins framework modified with a multicentered multipole expansion method for the electrostatic and polarization components. The multipole expansion is taken at every atomic center in order to calculate the interaction energy of the molecular pair of the arbitrary shaped molecules. The theoretical approach is briefly described below.

The Hamiltonian of the pair of the molecule is written as

$$H = (H^{(a)} + H^{(b)}) + H', \tag{1}$$

where $H^{(a)}$and $H^{(b)}$ are the Hamiltonians of the free molecules a and b, H' is the interaction term of the molecular pair. H is the total Hamiltonian of the molecular complex containing the n electrons of the molecule a and the m electrons of the molecule b.

H' is the perturbation operator; the molecular wave function is written in the form of the Slater determinant constructed by the constituent's atomic orbitals. The ground state molecular wave function of the molecule a is written as

$$\Psi_0^{(a)} = \frac{1}{\sqrt{n}} \det \left| \Psi_1^{(a)}(1)\Psi_2^{(a)}(2)\ldots\ldots\ldots\ldots\Psi_{\mathrm{n}}^{(a)}(n) \right|. \tag{2}$$

$\Psi_{\mathrm{n}}^{(a)}$(n) are the spin orbitals of in molecule a. The molecular orbital for molecule b is similarly defined as

$$\Psi_0^{(b)} = \frac{1}{\sqrt{m}} \det \left| \Psi_1^{(b)}(n+1)\Psi_2^{(b)}(n+2)\ldots\ldots\ldots\ldots\Psi_{\mathrm{m}}^{(a)}(n+m) \right|. \tag{3}$$

H' is treated as the perturbation operator and Rayleigh–Schrödinger perturbation method considers the ground state eigenfunction of $H^{(a)} + H^{(b)}$ as the product of $\Psi_0^{(a)}\Psi_0^{(b)}$. The perturbed wave function may be expressed in terms of unperturbed state by standard quantum mechanical theory.

To apply the perturbation on arbitrary shaped molecule, one can define the local charge density operator associated with two molecules. These operators are the functions of the electronic coordinates while the nuclear coordinates are kept fixed. Thus, the matrix element $\langle \Psi_0^{(a)}\Psi_0^{(b)} | H' | \Psi_0^{(a)}\Psi_0^{(b)} \rangle$ is simply written as the electrostatic interactions between the two charge densities. The electrostatic interactions between these distributions will be obtained with sufficient accuracy by replacing the continuous part of charge distribution by appropriate multipole expansions at every atomic center (or bond). This allows a considerable conceptual and computational simplification. The mean charge distribution function of the molecule is defined as

$$\left(f_{00} = \sum_{\mu} Z(\vec{r} - \vec{r}_{\mu}) - \sum_{\delta}\sum_{\gamma} p_{\delta\gamma}\chi_{\delta}^{*}(\vec{r})\chi_{\gamma}(\vec{r}) \right),$$

i.e., the sum of the nuclear point charge and the electronic distributions. The χ_δ and χ_γ are the atomic orbitals. The evaluation of the term $\sum_{\delta}\sum_{\gamma} p_{\delta\gamma}\chi_{\delta}^{*}(\vec{r})\chi_{\gamma}(\vec{r})$ is carried out by Mullkens' or Lowdin's method. The necessary formulas for the intermolecular interaction are given in the following section.

2.2.1 *Electrostatic Interaction Energy.*

$$E_{el} = E_{qq} + E_{qm} + E_{mm}. \tag{4}$$

E_{qq} represents the monopole–monopole interaction, while E_{qm} and E_{mm} correspond to monopole–dipole and dipole–dipole interactions, respectively.

2.2.2 Polarization Energy. The polarization energy, sometimes called as the induction energy, of a molecule (say a), is obtained as sum of induced polarizations for the various bonds involved:

$$E_{ind}^{(a)} = C\left(-\frac{1}{2}\right)\sum_{u} \vec{\varepsilon}_u^{[a]}\,\bar{A}_u^{(a)}\vec{\varepsilon}_u^{[a]}. \tag{5}$$

Here $\overline{\overline{\mathrm{A}}}_u$ is the polarizability tensor of the bond u and $\vec{\varepsilon}_u^{[a]}$ is the electric field created at this bond by the surrounding molecules other than (a). If the molecular charge distribution is represented by the atomic net charges, it is found that

$$\vec{\varepsilon}_u^{[a]} = \sum_{t\neq s}\sum_{\lambda}{}^{(b)} q_\lambda^{(b)} \bullet \frac{\vec{R}_{\lambda u}}{R_{\lambda u}^3}, \tag{6}$$

where $\vec{R}_{\lambda u}$ is the vector joining the atom λ in molecule (b) to the "center of polarizable charge" on the bond u of the molecule (s).

2.2.3 Dispersion and Short-Range Repulsion Energies. The dispersion and the short-range repulsion terms are given by the semiempirical formulas of a Lennard–Jones or a Buckingham type. The dispersion energy is always represented by $-\mathrm{A}/\mathrm{R}^6$ term, in agreement with the theoretical analysis. Kitaigorodskii adopted the "6-exp" potential and later on modified the parameters to suit all types of molecular systems. Accordingly,

$$E_{disp} + E_{rep} = \sum_{\lambda}{}^{(a)}\sum_{\nu}{}^{(b)} E(\lambda, \nu),$$

where

$$E(\lambda, \nu) = K_\lambda K_\nu\left(\frac{-A}{z^6} + Be^{-\gamma z}\right)$$

and

$$z = \frac{R_{\lambda\mu}}{R_{\lambda\nu}^0},\ R_{\lambda\nu}^0 = \sqrt{(2R_\lambda^w)(2R_\nu^w)}, \tag{7}$$

where R_λ^w and R_ν^w are the van der Waals radii of atoms λ and ν, respectively. The parameters A, B, and γ are not dependent on the atomic species: this necessary dependence is brought about by $R_{\lambda\nu}^w$ and by the factors K_λ, K_ν that allow the energy minima to have different values according to the atomic species involved [19].

These calculations generated a large amount of data that are summarized in supporting information (SI, available online) for space economy.

3. Results and Discussion

3.1 Geometry Optimization

The optimized geometries are given below with numbering scheme.

Abbreviation: Cr = crystal phase, Sm = smectic phase, N = nematic phase, I = isotropic phase.

It is obvious from Table 1 that the change in core group and in alkyl chain largely affects the phase sequences. A similar effect has been observed for other 2,5 disubsituted pyridine derivatives [17]. In the present work, we report the results of our investigation on the three types of pyridine molecules based on asymmetric interactions between a molecular pair.

3.2 Interaction Energy of Various Molecules and Their Phase Sequences

As we discussed in the introduction, the various interaction energies, i.e., stacking, in-plane and terminal energies are helpful to provide an insight into molecular behavior and formation of phase sequences. Here we summarize the interaction energies of all the studied molecules, and in SI Table 4 two parameters have been introduced: $\alpha = \frac{\text{Sum of stacking energies}}{\text{Sum of in} - \text{plane energies}}$ and $\beta = \frac{\text{Sum of terminal energies}}{\text{Sum of in} - \text{plane energies}}$. Here, sum refers to the sum of energies on both sides of the interacting molecule.

It may be observed from Table 2 that for the bipolar mesogens $\beta \approx 1$ and $\alpha > 2$ indicating that the terminal energies are comparable to the in-plane energies. The stacking energies are much higher in magnitude compared with the in-plane energies. Hence, as pointed out earlier after disruption of the crystal, alignment of the molecules through stacking and terminal interaction is possible. In the case of pyridine derivatives PD-3, $\alpha > 2$ and $\beta \ll 1$ thus for non-polar molecules, terminal interactions are not of much importance. For PD-1 and PD-2 the value of α is less than 2, while the value of β is 0.5 for PD-1 and negligible for PD-2. The terminal interactions are very weak in the case of the selected pyridine derivatives. The alignment of the molecules is mainly due to stacking interactions.

3.3 Inter Molecular Interaction Energies Calculations for Polar Mesogens

3.3.1 H6CBP and H6NBP. Both of the molecules have polar groups at both ends. The total terminal interaction energies (SI Tables 1.1 and 2.1) are comparable to the in-plane interaction energies. The electrostatic part of the terminal interaction energies for both molecules is comparatively high, so the molecules are capable of forming a long chain through terminal interactions.

It is to be noted that in all the interaction configurations for H6CBP (SI Figure 1.1), the interaction energy is calculated for all possible variations, i.e., flipping the interacting molecule about the X-axis and translating the molecule along all three axes. The results have been reported as obtained after refinement. For antiparallel stacking (configuration 1) alkoxy chains and hydroxyl groups are having close interactions with biphenyls of the other molecules. In parallel stacking (configuration 2), alkoxy chains and hydroxyl groups are interacting with each other extending up to one benzene ring of the biphenyl. In the case of the in-plane interactions, parallel interactions are not favorable. In configuration 3, the alkoxy oxygens face each other and hence shift the interacting molecules toward an imbricated structure. In configuration 4, the O- - -O repulsion is reduced and hence alkoxy chains and hydroxyl groups interact with the biphenyl part of the other molecule. In configuration 5 of terminal interactions, hydroxyl groups of each molecule form hydrogen bonds with the other and in configuration 6 the cyano groups exhibit a dipolar interaction giving extra stability as was pointed out by Zugenmaier [19]. Thus, the terminal interactions in both cases are strong enough to form an extended chain of the molecules.

For both antiparallel and parallel stacking interactions, translation along the X-axis is allowed for a short range for H6CBP molecules (Fig. 1(a)). However, antiparallel stacking allows translation without expense of much energy and hence is able to maintain nematic order for a considerable range of temperature while parallel stacking is relatively more specific and is liable to dissociate at increasing temperature. In the case of in-plane interactions, H6CBP molecules also have freedom to translate along the X-axis for a short

Table 1. Compounds with optimized geometry, phase sequences, important dihedrals and dipole moments

Name	Compounds optimized structure with numbering scheme	Phase Transition Temperature (°C) & Phase Type	Dihedral angle between the plane of two rings	The dipole Moment & its components along X,Y,Z axis
H6CBP	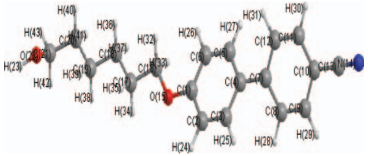	(Pure nematic) Cr_1 94.8 N 110.3 I Cr_2 91.9 N 110.3 I I 110 N 80-82 Cr_1 (Cooling)	35.62°.	7.25 debye (X: −5.80; Y: −1.81; Z: −3.94)
H6NBP	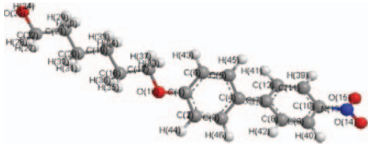	(Pure nematic)	325.14°	6.89 debye (X: −6.39; Y: 0.24; Z: −2.55)
PD-1	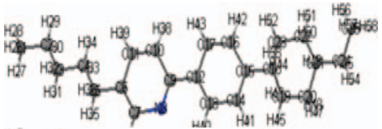	Cr-40.2-Sm-84.6-N-153.1-I Both smectic & nematic for wide range	0.95	1.68 debye (X: −1.1297 Y: 1.2489 Z: 0.0165)
PD-2	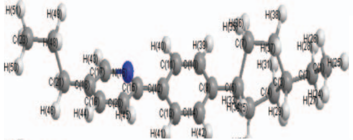	Cr-51-Sm-94-N-157.8-I Both smectic & nematic for wide range	15.49°	1.94 debye (X: −1.34; Y: 1.20; Z: 0.70)
PD-3	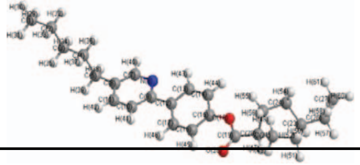	Cr-116-N-173.5-I Pure nematic although length breadth ratio is large	15.96°	1.97 debye (X: 0.79; Y: 0.80; Z: 1.97)

Table 2. Variation of phase sequences along with variation in α and β parameters

S.No.	Name of Molecule	Sum of the two stacking side energies (kcal/mol)S	Sum of the two in-plane side energies (kcal/mol)P	Sum of the two terminal side energies (kcal/mol)T	$\beta = \frac{T}{P}$	$\alpha = \frac{S}{P}$	Phases
1	H6CBP	42.3	20.2	20.3	1.005	2.09	N
2	H6NBP	69.0	29.5	29.1	0.99	2.34	N
3	PD-1	43.4	28.1	1.4	0.50	1.54	SN
4	PD-2	42.2	26.8	5.3	0.198	1.57	SN
5	PD-3	47.0	16.7	4.8	0.287	2.81	N

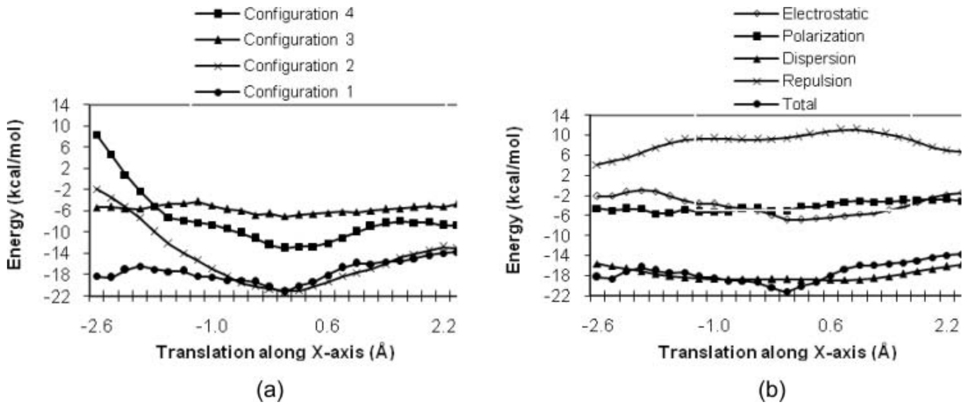

Figure 1. (a) Variation of interaction energy with translation along X-axis during interactions under various configurations of H6CBP. (b) Variation of interaction energy components with translation along X-axis during anti-parallel stacking interactions under configuration 1 of H6CBP.

range, although configuration 4 appears to be more stable than configuration 3. In the case of terminal interactions, H6CBP molecules have freedom to rotate about the X-axis, but it should be noted that since they are strongly bound due to stacking through in-plane and terminal interactions, such rotations might not be possible. SI Figure 1.1 shows that the stacked molecules will be linked by terminal interactions, irrespective of their relative orientations and hence the crystal energy will be quite high resulting in a relatively high melting point.

The lowest energy configurations for H6NBP is (SI Figure 2.1) obtained where both stacking interactions are antiparallel. Configuration 2 shows better overlap, and hence is lower in energy. In-plane interactions are also antiparallel, and as expected, configuration 4 with alkoxy oxygens receding from each other possesses lower energy than configuration 3 where the alkoxy oxygens are facing each other. Terminal interactions are strong due to hydrogen bonding between the hydroxyl group and NO_2 group at the ends. The other configurations of terminal interactions are much less favorable, although the possibilities of hydroxyl–hydroxyl terminal interaction cannot be ruled out.

Figure 2(a) shows the variation of interaction energy components with translation about the X-axis for different configurations of a pair of H6NBP molecules. During stacking interactions, translation along the X-axis is allowed for a short range while in the case of in-plane side interactions of H6NBP molecules, the freedom to translate along the X-axis is slightly greater. In the case of terminal interactions, the molecules have freedom to rotate along the X-axis.

Both bipolar mesogens chosen for this study are of reasonably good length to breadth ratio. These molecules have a natural tendency for alignment as dispersion forces increase with the extent of overlap. Obviously, a major contribution toward the interaction energy comes from dispersion. However, dispersion alone cannot dictate mesogenic character, since in a large assembly of molecules, one molecule may partially overlap with more than one molecule contributing to a large dispersion energy. The necessary selectivity arises due to electrostatic interactions. From Figs 1(b) and 2(b), it may be observed that the dispersion maintains a constant value with respect to small variations for the configuration 1, and it is true for all the configurations unless there is a short contact where dispersion energy increases but the total energy is compensated by an increase in repulsion energy. It is also true for polarization energy. The electrostatic energy shows a minimum, which is carried on to the total energy. It may be concluded that a specific minimum is guided by the electrostatic part of interaction while the dispersion energy makes it stable. The allowance of translation along the long molecular axis with small expense of energy permits the nematic flow.

As the bipolar mesogens exhibit a tendency to form long chains through terminal interactions, the crystal structures are tightly packed. The in-plane interaction energies are comparable to the terminal interaction energies, hence it is expected that when the temperature is increased both in-plane interactions as well as terminal interactions will be disrupted almost simultaneously giving rise to a nematic phase. However, a tight packing also indicates a relatively high melting point, which is observed in such systems.

It is to be further noted that a smectic character necessarily involves layer formation, where the layers can slide over each other. Such layers may be formed either due to stacked in-plane interactions or due to imbricated stacked configurations. In the former case, the terminal interactions must be weak while in the latter case the in-plane interactions should be smaller in magnitude compared with the stacking. The studied molecules H6CBP and H6NBP both show reasonably good overlapping at minimum energy stacked configurations hence not favoring imbricated stacking. The in-plane interaction energy is less than half of the value of the preferred stacked configuration energy. Hence, such molecules do not give an indication of forming smectic layers.

3.4 Interaction Energy Calculation for 2,5 Disubsituted Pyridine-Derivatives

3.4.1 PD-1. From SI Table 3.1 it is clear that dispersion is a major contribution whereas repulsion provides some compensation for it. The interaction energy of the in-plane configuration 4 for PD-1 is comparable in magnitude to the stacking energy of configuration 1. This is probably due to the non-planarity of the molecule at the cyclohexane part. The non-planarity makes stacking interactions (configuration 1) and in-plane interactions (configuration 4) almost equivalent. The lower energy in stacking configuration 2 and in-plane configuration 3 means they are not preferred configurations. The total energies in case of

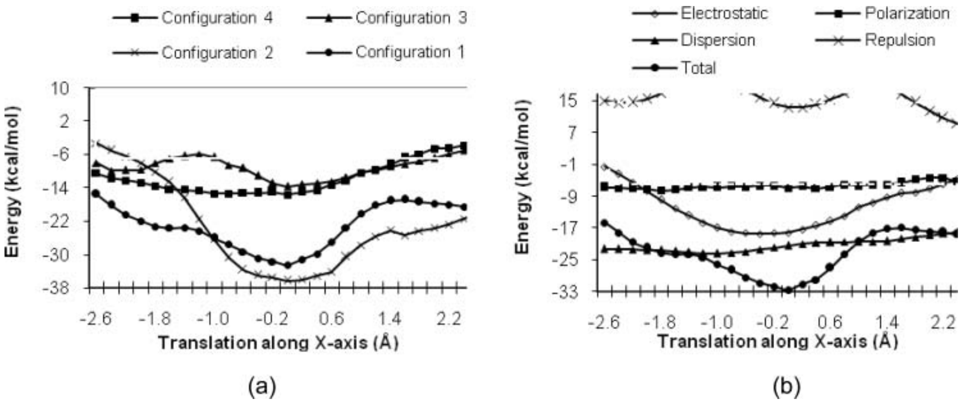

(a) (b)

Figure 2. (a) Variation of interaction energy components with translation along X-axis during stacking interactions under various configurations of H6NBP. (b) Variation of interaction energy components with translation along X-axis during stacking interactions under configuration 1 of H6NBP.

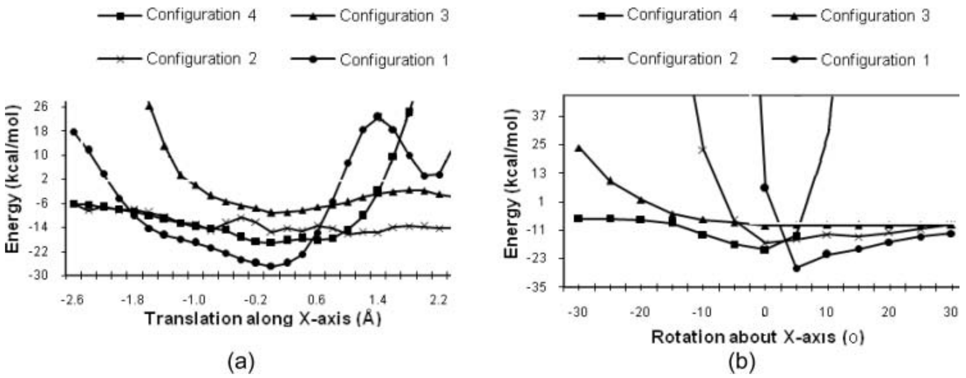

Figure 3. (a) Variation of interaction energy components with translation along X-axis during stacking interaction under configuration 1 for PD-1 molecules. (b) Variation of interaction energy components with rotation about X-axis during stacking interaction under configuration 1 for PD-1 molecules.

terminal interactions are much lower in magnitude than that of stacking interactions and in-plane interactions.

The SI Figures 3.1 (a)–(f) show the lowest energy configurations of the pairs of PD-1 molecules. In stacking configuration 1, the pyridine ring of one molecule is perpendicular to the cyclohexane of the second molecule and both molecules interact in an antiparallel manner. In stacking configuration 2, molecules are shifted with respect to each other so that the in-plane parts interact leaving the non-in-plane part aside. In case of the in-plane interactions at configuration 3, the pyridine rings of both molecules interact closely with each other and ethyl groups interact with the benzene rings. In the case of the in-plane interactions with configuration 4, the pyridine rings face away from one another and pyridine ring of each molecule interacts with the benzene ring of the other whereas the ethyl group interacts with the cyclohexane. In the terminal interactions with configuration 5, the ethyl group of each molecule interacts with that present in the other. In the terminal configuration 6, the ethyl chain of one molecule has an interaction with the alkyl chain of the second molecule.

Figures 3(a) and (b) show the variation of the interaction energy components with translation and rotation about the X-axis for different configurations of a pair of PD-1 molecules. In stacking the interactions, translation along the X-axis as well as rotation about the X-axis is restricted. In case of the in-plane interactions of PD-1, the molecules have freedom to translate along the X-axis as well as rotate about the X-axis for a short range in one direction only.

3.4.2 PD-2. In this case, the dispersion energy is a major contribution whereas repulsion provides compensation for it (SI Table 4.1). The sum of in-plane energy for PD-2 is comparable in magnitude to the individual stacking energy at any side. This reflects a tendency for smectic with nematic character. The total energy in the case of terminal interactions is much lower than that of stacking or in-plane interactions.

In the stacking configuration 1 (SI Figures 4.1 (a)–(f)), the cyclohexane of each molecule has closer interactions with the benzene rings of other molecules, and the propyl groups interact with the pyridine rings of each other. In the stacking configuration 2, the second molecules flips over bringing the propyl group of the second molecule close to

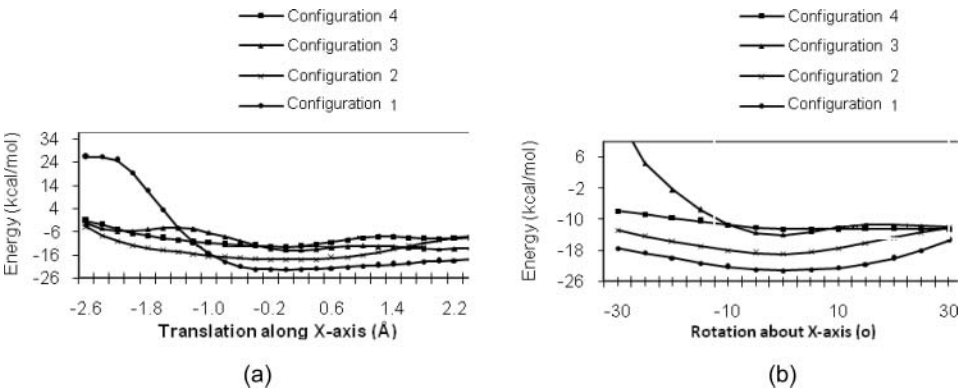

Figure 4. (a) Variation of interaction energy with translation along X-axis during interaction under various configuration for PD-2 molecules. (b) Variation of interaction energy with rotation along X-axis during interaction under various configuration for PD-2 molecules.

cyclohexane of the first. In the case of the in-plane configuration 3, the pyridine rings of both molecules interact with the cyclohexane of the other molecule while the benzene rings and the alkyl chain interact with similar parts of the other molecule. In case of in-plane interactions shown in configuration 4, the second molecule interacts from the other side; the pyridine ring of each molecule interacts with the benzene ring of the other, whereas the propyl chain interacts with the cyclohexane. In the terminal configuration 5, the alkyl chain of each molecule interacts with that in the other molecule. In the terminal configuration 6, the propyl chain of one molecule has interactions with the alkyl chain of the second molecule.

For the stacking interaction at configuration 1 (Figs 4(a)–(b)), translation along the X-axis is allowed for a short range, in one direction, with a very limited rotation about the X-axis. In the stacking configuration 2, translation as well as rotation about the X-axis is allowed for a short range. In the case of in-plane interactions of PD-1, the molecules have restricted freedom to translate along the X-axis as well as rotate about the X-axis for a short range. It may be noted that due to non-planarity of the cyclohexane in both PD-1 and PD-2, the stacking and the in-plane interaction energies are comparative hence making layer formation easier. Further, the two-stacked configurations are quite different in nature. For example configuration 1 of PD-2 is antiparallel while configuration 2 is parallel.

3.4.3 PD-3. The total energies (SI Table 5.1) in case of terminal interactions are much lower in magnitude than that of stacking interactions and in-plane interactions. This suggests that molecules are aligned mainly due to stacking interactions and the layers are free to slide over each other.

SI Figures 5.1 (a)–(f) show the lowest energy configurations of pairs of PD-3. This molecule possesses a bent structure with a long alkyl chain at one end and a cyclohexane with an ethyl group at the other. In the stacking configuration 1, the alkyl chain of each molecule has close interaction with the oxo group as well as the benzene ring of the other molecule. For the stacking configuration 2 the cyclohexane of each molecule has close interaction with the benzene as well as the pyridine rings of the interacting molecules. In the case of in-plane configuration 3, the pyridine ring of both molecules interact with the alkyl chains of the other molecule. In the case of in-plane configuration 4, parallel

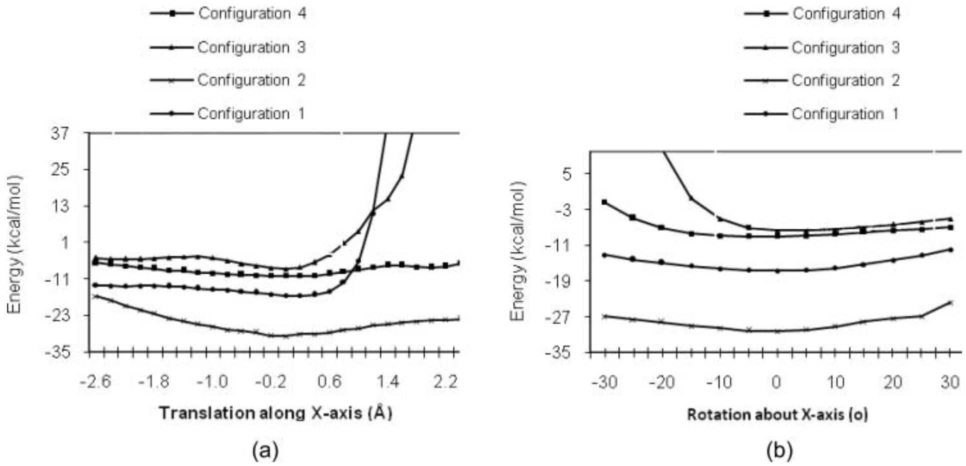

Figure 5. (a) Variation of interaction energy with translation along X-axis during interaction under various configuration for PD-3 molecules. (b) Variation of interaction energy components with rotation about X-axis during interaction under various configuration for PD-3 molecules.

interactions of all the components are observed. In configuration 5 of terminal interactions, the alkyl chains of one molecule interact with the ethyl group of the other molecule while in configuration 6 the alkyl groups of both molecules interact with each other.

It can be seen from SI Figs 5(a) and (b) that in the stacking interaction, translation along the X-axis is allowed for a very short range in one direction, with a limited rotation about the X-axis, since the presence of the cyclohaxane restricts the complete overlap of the molecules. In the stacking configuration 2, translation as well as rotation about the X-axis is allowed for a short range. In the case of in-plane configuration 3, translation along the X-axis is allowed for a short range in one direction and rotation about the X-axis is highly restricted. In the case of in-plane interaction (configuration 4) of PD-3, the molecules have freedom to translate along the X-axis as well as to rotate about the X-axis for a short range.

As discussed in the introduction, the pyridine derivatives were chosen with a view to examining the mesogenic character on the basis of energy considerations. PD-1 and PD-2 are of wide smectic range and nematic range. PD-3 is purely a nematogen despite having a molecular length comparable to PD-1 and PD-2. The broad outcome of energy considerations at various configurations are summarized below.

1) For non-polar long chain molecules, the stacking energy seems to be a measure of nematic character. Stronger stacking favors alignment of molecules, which may be retained after disruption of the crystal.
2) In-plane interaction plays a significant role in deciding smectic character. If the in-plane interaction is strong and approaches almost 50% of the stacking energy, smectic character develops. This is probably due to the increased possibilities of layer formation through in-plane interaction. If stacked configurations are dissimilar in nature for opposite side of the molecule, the layers are movable and hence displaying smectic character for a wide range.
3) Non-planarity allows the stacked and in-plane pairs to be comparable in energy hence increasing smectic character as was observed in case of pyridine derivatives.

4) PD-3 molecule, although longer in length and non-plane in structure, is nematic because the in-plane interaction is weak.
5) Terminal interaction, in case of molecules with non-polar end, is generally weak and hence allows the crystal to disrupt before attaining a complete disorder.
6) It was also noticed that for stacking and in-plane interactions, the type of alignment, i.e., whether parallel or antiparallel is also an important feature. A careful observation shows that a layer formation is possible if molecules are available in a systematic sequence. The crystal structure vis-à-vis preferred configuration may serve as a guideline for this purpose.

4. Conclusion

The specificity of the interactions is the primary consideration as it helps to understand the freedom of molecules to translate or rotate in any direction. If freedom increases, no matter what the energy ratio be, neither stacking nor layer formation remains stable. The selectivity of configurations is mainly due to the electrostatic energy, which is effective over the longest range. Once the molecule comes closer at the specific orientation, other forces come into play (especially dispersion) and the binding becomes stronger. The molecule gradually acquires the final configuration avoiding the short contacts. The electrostatic part of the terminal interaction energy may some times be even stronger than that in stacking although. The total energy of stacking interaction is much higher in magnitude than other type of interactions. Thus, dimer formation through terminal association is a natural consequence. As the total energies in the case of terminal and in-plane interactions are comparable, only orientational order due to strong stacking remains after disruption of the crystal structure. The material therefore behaves as nematic mesogens. A rough measure of nematic character may be assigned to the facts that the sum of in-plane energies on both side of the molecules is less than or even comparable to the most preferred stacking energy, the mesogenic character is nematic.

However, a more detailed investigation related to the interaction energy at various configurations may provide new feature which has not been understood so for.

Acknowledgment

The authors are thankful to the Department of Science & Technology for providing the computational facilities under DST-FIST Grant No SR/FST/PSI/087/204.

References

[1] de Gannes, P. G., & Prost, J. (1993). *Physics of Liquid Crystals,* 2nd ed., Oxford University Press: Oxford.
[2] Dunmur, D. A., & Singh, S. (2002). *Liquid Crystals*, World Scientific: Singapore.
[3] Priestley, E. B., Wojtowicz, P. J., & Sheng, P. (1975). *Introduction to Liquid Crystals*, Plenum Press: New York & London.
[4] Roychoudhury, M., & Thakur, S. K. (2011). *Mol. Cryst. Liq. Cryst.*, *548*, 1.
[5] Roychoudhury, M., Thakur, S. K., & Gaurav, P. (2011). *J. Molecular Liquids*, *161*, 55.
[6] Roychoudhury, M., & Kumar, D. (1996). *Materials Sci. Forum Transtec Publ. Switzerland*, *13*, 222.
[7] Onsager, L. (1949). *Ann. N. Y. Acad Sci.*, *51*, 627.
[8] Maier, W., & Saupe, A. (1958; 1959; 1960). *Z. Naturforsch. A13*, 564; *A14*, 882; *A15*, 287.
[9] Luckhurst, G. R., Zannoni, C., Nordio, P. L., & Segre, U. (1975). *Mol. Phys.*, *30*, 1345.

[10] Sheng, P. (1975). Introduction continuum theory of liquid crystals. In: P. Sheng, E. B. Priestley & P. J. Wojtowicz (Eds.), *Introduction to Liquid Crystals*, Plenum Press: New York & London.

[11] McDonald, A. J., & Hanna, S. (2004). *Mol. Cryst. Liq. Cryst.*, *413*, 2271.

[12] McDonald, A. J., & Hanna, S. (2006). *J. Chem. Phys.*, *124*, 164906.

[13] Pelaez, J., & Wilson, M. R. (2006). *Phys. Rev. Lett.*, *97*, 267801.

[14] Petrove, V. F., & Pavluchenko, A. I. (2002). *Mol. Cryst. Liq. Cryst.*, *383*, 63.

[15] Tiberio, G., Muccioli, L., Berardi, R., & Zannoni, C. (2009). *Chem. Phys. Chem.*, *10*, 125.

[16] Siegbahn, P. E. M. (2003). *Quaet. Rev. Biophys.*, *36*, 91.

[17] Zugenmair, P. (2002). *Liq. Cryst.*, *29*, 443.

[18] Gaussian 03, Revision D.01, Frisch, M. J., Trucks, G. W., Schlegel, H. B., Scuseria, G. E., Robb, M. A., Cheeseman, J. R., Montgomery, J. A. Jr., Vreven, T., Kudin, K. N., Burant, J. C., Millam, J. M., Iyengar, S. S., Tomasi, J., Barone, V., Mennucci, B., Cossi, M., xScalmani, M., Rega, N., Petersson, G. A., Nakatsuji, H., Hada, M., Ehara, M., Toyota, K., Fukuda, R., Hasegawa, J., Ishida, M., Nakajima, T., Honda, Y., Kitao, O., Nakai, H., Klene, M., Li, X., Knox, J. E., Hratchian, H. P., Cross, J. B., Bakken, V., Adamo, C., Jaramillo, J., Gomperts, R., Stratmann, R. E., Yazyev, O., Austin, A. J., Cammi, R., Pomelli, C., Ochterski, J. W., Ayala, P. Y., Morokuma, K., Voth, G. A., Salvador, P., Dannenberg, J. J., Zakrzewski, V. G., Dapprich, S., Daniels, A. D., Strain, M. C., Farkas, O., Malick, D. K., Rabuck, A. D., Raghavachari, K., Foresman, J. B., Ortiz, J. V., Cui, Q., Baboul, A. G., Clifford, S., Cioslowski, J., Stefanov, B. B., Liu, G., Liashenko, A., Piskorz, P., Komaromi, I., Martin, R. L., Fox, D. J., Keith, T., Al-Laham, M. A., Peng, C. Y., Nanayakkara, A., Challacombe, M., Gill, P. M. W., Johnson, B., Chen, W., Wong, M. W., Gonzalez, C., & Pople, J. A. (2004). Gaussian, Inc.: Wallingford, CT.

[19] Claverie, P. (1978). Elaborations of approximate formulas for interactions between large molecules: Applications in organic chemistry. In: B. Pullman (Eds.), *Inter Molecular Interactions from Diatomic to Biopolymers*, J. Wiley & Sons Ltd.: Hoboken, NJ, 217–226.